WALAILAK JOURNAL
http://wjst.wu.ac.th Engineering and Physical Sciences

Closed-Loop Input Shaping with Quantitative Feedback Controller Applied to Slewed Two-Staged Pendulum

Withit CHATLATANAGULCHAI[*] and Takat BENJALERSYARNON

Department of Mechanical Engineering, Faculty of Engineering, Kasetsart University, Bangkok 10900, Thailand

([*]Corresponding author's e-mail: fengwtc@ku.ac.th)

Received: 28 March 2015, Revised: 11 October 2015, Accepted: 17 November 2015

Abstract

In this paper, 2 practical techniques for control of dynamic systems are integrated. An input shaper is placed outside of a closed-loop system to reduce vibrations induced by the reference input. A quantitative feedback controller handles the vibrations induced by disturbances and noise while ensuring good tracking and stability. They are practical because designing an input shaper only requires knowledge of natural frequencies and damping ratios of the system whereas a quantitative feedback controller lets the designer quantitatively evaluate tradeoffs among tracking, disturbances and noise rejections, and stability among others. Various frequency-domain specifications are combined for the controller to meet requirements for all plants in an uncertain plant set. The proposed control system is applied to a 2-staged pendulum to suppress residual vibration from point-to-point movement.

Keywords: Closed loop, input shaping, quantitative feedback, vibration reduction, two-staged pendulum

Introduction

Input shaping was proposed by [1], based on the Posicast control idea from [2,3]. The technique combines the input to the system with a sequence of impulses, whose amplitudes and timing are optimally designed such that the shaped input avoids exciting the natural modes of oscillation of the underdamped system. The result is the reduction of unwanted transient deflection and residual vibration in the system. An excellent review of the input shaping technique can be found in [4].

Input shaping, even though viewed as an open-loop technique, is rarely implemented without a closed-loop controller. The input shaper is either placed inside or outside of the feedback controller loop. When placed inside, the input shaper reduces vibration by preventing the system from being excited by reference, disturbances, and noise. When placed outside, the input shaper reduces vibration from a reference signal. The closed-loop controller is duty bound to provide accurate tracking and good disturbances and noise rejections, amidst model uncertainty. Recent works on closed-loop input shaping can roughly be split equally between placing the input shaper inside and outside of the feedback loop.

Some notable works that place the input shaper inside of the feedback loop include: 1) Huey and Singhose [5] who used root locus to show that the closed-loop system, consisting of an input shaper placed inside of the loop and a simple P, PID, or lead controller, susceptible to instability; 2) Stergiopoulos and Tzes [6] applied a robust controller to the feedback loop with the input shaper placed inside. The controller addresses the uncertainty of the plant transfer function's denominator, while ensures accurate tracking; 3) Kapila *et al.* [7] used full state-feedback controller to provide stability to the time-delay system which results from placing the input shaper inside the loop. The controller gain is synthesized based on the Riccati equation and LMI approach; 4) Staehlin and Singh [8] applied the internal model control (IMC) idea in their design. The feedback controller consists of the input shaper in the feedforward path and the plant transfer function in the feedback path around the input shaper. As a

result, the output of the feedback controller to the plant is the same as that of the open-loop input shaper. Stability is analyzed when the plant transfer function has uncertainty; 5) Zuo and Wang [9] used inverse dynamics to cancel the rigid part of the plant to leave only the flexible part. A PD controller and an input shaper are placed inside of the loop.

Some notable works that place the input shaper outside of the feedback loop include: 1) Zolfagharian *et al.* [10] used a PD and an iterative learning controller in the feedback loop. A genetic algorithm was used to adjust their gains to provide robustness. Similar ideas can be found in [11]; 2) Pai [12] and Hu *et al.* [13] independently used a sliding mode controller in the feedback loop to make the closed-loop system behave like a reference model. An input shaper was then designed to suppress vibration of the reference model; 3) Huey and Singhose [14] and Kenison and Singhose [15] used a PD in the feedback loop. They concurrently designed the PD gains and the input shaper parameters simultaneously for a simple plant by taking into account limits on allowable overshoot, residual vibration, and actuator efforts; 4) Dharne and Jayasuriya [16] used an adaptive scheme to adjust the feedback controller so that the closed-loop flexible poles converge to those of the plant.

This paper shows that placing the input shaper inside of the feedback loop can reduce vibrations induced by reference input, plant-input and plant-output disturbances, and noise. However, the time delay and non-minimum phase introduced by the input shaper may limit performance of the control system by imposing lower bounds on the closed-loop transfer functions' magnitude or may make designing a good feedback controller difficult due to constraints on bandwidth.

In this paper, placing the input shaper outside of the feedback loop is investigated. The input shaper is charged only to reduce vibration caused by reference input, whereas the quantitative feedback controller handles vibrations caused by other sources. Two advantages from using the quantitative feedback controller are as follows: 1) the controller explicitly and quantitatively takes plant model uncertainty into account during the control design process. Therefore, the control system performance in suppressing the vibrations can be guaranteed despite having plant uncertainty; 2) the controller enforces frequency-domain specifications on tracking and disturbances and noise rejections. Therefore, vibrations caused by plant-input and plant-output disturbances and noise are attenuated, while good tracking is assured. The proposed control system is simulated on an underdamped second-order plant. Both simulation and experiment on a 2-staged pendulum are presented.

Closed-loop input shaping

The input shaper can be implemented in the closed-loop system either by placing the input shaper inside of the loop (as shown in **Figure 1**) or outside of the loop (as shown in **Figure 2**). Using the terms given by [17], the former is called closed-loop signal shaping (CLSS) and the latter is called outside-the-loop input shaping (OLIS). In **Figure 1**, *P* is the underdamped plant, *NL* represents hard nonlinearities (backlash, deadzone, saturation, and hysteresis), *IS* is the input shaper, *C* is the feedback controller, *n* is noise, *y* is the measured output, d_O is the plant-output disturbance, *f* is the output from the nonlinearities, d_I is the plant-input disturbance, $\bar{u}$ is the output from the input shaper, *u* is the output from the controller, *e* is the tracking error, and *r* is the reference. In **Figure 2**, r is the shaped reference from the input shaper and $\bar{r}$ is the original reference.

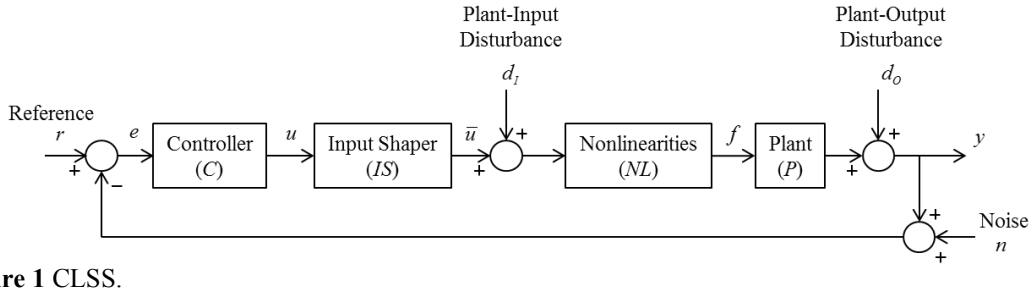

Figure 1 CLSS.

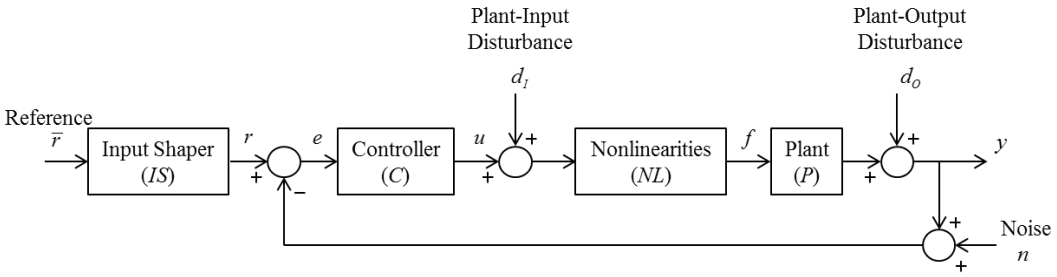

Figure 2 OLIS.

For an underdamped plant P, having complex poles, residual vibrations, as appear in y, are caused by: 1) reference r; 2) plant-input disturbance d_I; 3) plant-output disturbance d_o; and 4) measurement noise n.

Three other common sources of vibrations are initial conditions, hard nonlinearities, and plant model uncertainty.

The effect of initial conditions can be included in the plant-output disturbance d_o as can be seen from the Laplace transformation of an underdamped plant P with non-zero initial conditions, given by;

$$Y(s)=\frac{F(s)}{ms^2+cs+k}+\frac{(ms+c)y(0)+m\dot{y}(0)}{ms^2+cs+k}+D_O(s). \tag{1}$$

Hard nonlinearities cause vibrations by altering the designed input to the plant. The designed input, either from the controller or the input shaper, aims to subdue vibrations, so altering it leads to uncontrolled vibrations. Hard nonlinearities must be accounted for in the control algorithm either to ensure they will not alter the designed plant input or to be sure their effects are still within the design specifications. Because the controller and the input shaper were designed on a fixed plant model, if there is uncertainty in the plant model, either due to imperfect system identification or time-varying plant, the control system performance in suppressing the vibrations may degrade.

CLSS: Advantages

Placing the input shaper inside of the loop as shown in **Figure 1** has the advantage that the input shaper helps reduce vibrations caused by reference, plant-input disturbance, plant-output disturbance, and noise. A simulation study can readily be performed to confirm this fact.

With an underdamped plant of the form $P(s)=\omega_n^2/\left(s^2+2\zeta\omega_n s+\omega_n^2\right)$, where $\omega_n=1$ rad.s^{-1} and $\zeta=0.1$; a PID controller with $k_p=1$, $k_i=0.5$, and $k_d=0.1$; an input shaper with 3 impulses, given by;

$$IS(s)=F_0+F_1z^{-t_1}+F_2z^{-t_2}, \tag{2}$$

where $F_0=1/\left(1+2K+K^2\right)$, $F_1=2K/\left(1+2K+K^2\right)$, $F_2=K^2/\left(1+2K+K^2\right)$, $K=e^{-\zeta\pi/\sqrt{1-\zeta^2}}$, $t_1=\pi/\left(\omega_n\sqrt{1-\zeta^2}\right)$, $t_2=2\pi/\left(\omega_n\sqrt{1-\zeta^2}\right)$, and $z^{-1}=e^{-st_s}\approx 1-t_s s$, where t_s is the sampling period; and neglecting the nonlinearities, the simulation results, from simulating the block diagram in **Figure 1**, for various unit-step inputs, with and without input shaping, are shown in **Figure 3**.

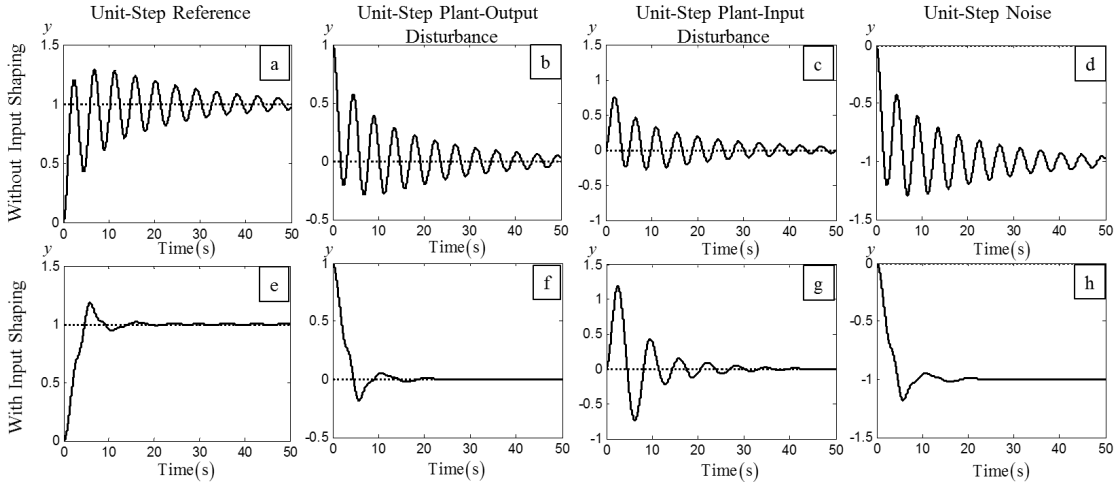

Figure 3 Simulation of CLSS. a) to d) are the outputs *y* due to unit-step reference, unit-step plant-output disturbance, unit-step plant-input disturbance, and unit-step noise, respectively, without input shaping. e) to h) are those with input shaping. The solid lines are the output *y*, and the dotted lines are the reference *r*.

Figure 3a is when a unit-step reference *r* is given while other inputs are zero. It is without input shaping. The solid line is the output *y*, and the dotted line is its reference *r*. **Figure 3b** is similar but with only unit-step plant-output disturbance d_O is given while other inputs are zero. **Figure 3c** is with only unit-step plant-input disturbance d_I. **Figure 3d** is with only unit-step noise *n*. **Figures 3e** - 3**h** are those results with input shaping. It is clear that the input shaper helps reduce vibrations from various sources.

This fact can also be proved by inspecting the magnitude of the transfer functions from various inputs to the output, given by (3) - (5);

$$\left|\frac{Y(s)}{D_O(s)}\right| = \left|\frac{1}{1+P(s)IS(s)C(s)}\right|, \tag{3}$$

$$\left|\frac{Y(s)}{D_I(s)}\right| = \left|\frac{P(s)}{1+P(s)IS(s)C(s)}\right|, \tag{4}$$

$$\left|\frac{Y(s)}{N(s)}\right| = \left|\frac{Y(s)}{R(s)}\right| = \left|\frac{P(s)IS(s)C(s)}{1+P(s)IS(s)C(s)}\right|. \tag{5}$$

The input shaper (IS) can then cancel the effect of the underdamped poles of the plant *P* in all transfer functions, resulting in less vibration. Note that for convenience we only show the result of the SISO case and neglect the nonlinearities (NL). Note also that the feedback controller *C* can achieve the same vibration reduction results as those from the input shaper.

CLSS: Disadvantages

The input shaper usually has the form of an FIR filter $IS(s) = F_0 + F_1 z^{-t_1} + F_2 z^{-t_2} + ...,$ where F_i are the normalized impulse magnitudes, occurring at times $t_i,$ and because $z^{-1} = e^{-st_s} \approx 1 - t_s s,$ including the input shaper inside of the loop is equivalent to adding time delays, unstable zeros, or non-minimum phase to the plant. All of which may limit the performance of the control system or make designing the feedback controller difficult.

To show this fact, consider again the underdamped plant $P(s) = \omega_n^2 / \left(s^2 + 2\zeta\omega_n s + \omega_n^2\right)$ and the 3-impulse input shaper (2). From the block diagram in **Figure 1**, the open-loop transfer function is given by $L(s) = P(s)IS(s)C(s).$ Note that the input shaper adds a worst-case unstable zero of $s = 1/t_s$ or a time delay of $t_d = t_s t_2$ to *L*. For the closed-loop transfer functions, we have $e = Sr - Sd_O - SPd_I + Tn,$ where $S = 1/(1+L)$ and $T = L/(1+L).$

To suppress vibrations from *r* and $d_O,$ we want the H_∞ norm $\|S\|_\infty$ to be small. To suppress vibrations from *n*, we want $\|T\|_\infty$ to be small. To suppress vibrations from $d_I,$ we want $\|SP\|_\infty$ to be small. However, from Skogestad and Postlethwaite [18], with unstable zero, the lower bounds for $S,$ $T,$ and SP are given by $\|S\|_\infty \geq 1,$ $\|T\|_\infty \geq 1,$ and $\|SP\|_\infty \geq |P(s)|_{s=1/t_S}$. These lower bounds limit the performance of the feedback controller in rejecting disturbances and obtaining good tracking.

The bandwidth frequency for a system with time delay also has an upper bound $\omega_B < 1/(t_s t_2).$ It can be shown that for the system to have good performance at low frequencies (including good disturbances rejection and tracking), the bandwidth frequency must obey $\omega_B < 0.5/t_s$ and at high frequencies (including good noise rejection), the bandwidth frequency must be $\omega_B > 2/t_s.$ These bandwidth limitations make designing a good feedback controller difficult.

The unstable zero also leads to instability when using high feedback gain since as feedback gain increases toward infinity, the closed-loop poles move to the open-loop zeros. There may be more complications in designing the feedback controller in the case when the plant also has unstable poles or there is uncertainty in the plant model.

Outside-the-loop input shaping (OLIS)

Placing the input shaper outside of the loop as shown in **Figure 2** can only reduce vibrations caused by reference, not by disturbances and noise. This fact can be seen from the transfer functions, given by (6) - (9);

$$\left|\frac{Y(s)}{R(s)}\right| = \left|\frac{P(s)C(s)IS(s)}{1+P(s)C(s)}\right|, \tag{6}$$

$$\left|\frac{Y(s)}{D_O(s)}\right| = \left|\frac{1}{1+P(s)C(s)}\right|, \tag{7}$$

$$\left|\frac{Y(s)}{D_I(s)}\right| = \left|\frac{P(s)}{1+P(s)C(s)}\right|, \tag{8}$$

$$\left|\frac{Y(s)}{N(s)}\right| = \left|\frac{P(s)C(s)}{1+P(s)C(s)}\right|, \tag{9}$$

where the input shaper $IS(s)$ only appears in the transfer function from $R(s)$ to $Y(s)$. The controller C must take care of the other sources of vibrations. Nevertheless, not including the input shaper inside of the loop avoids adding time delays, unstable zeros, or non-minimum phase to the plant, which may allow the controller to work without limitations.

Closed-loop input shaping with quantitative feedback controller

In this section, we investigate placing the input shaper outside of the loop as in **Figure 2** and use a quantitative feedback controller (for more details, see [19]). **Figure 4** contains a diagram similar to that of **Figure 2**, but the feedback controller C is replaced by a quantitative feedback controller. The quantitative feedback controller consists of a prefilter F and a controller G. The controller G handles tracking and disturbances and noise rejection, while the prefilter F handles only tracking.

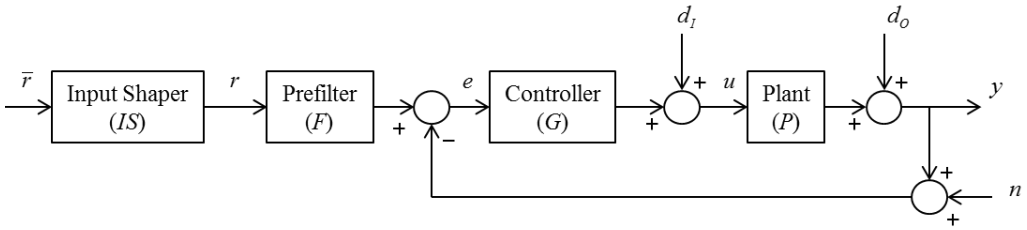

Figure 4 OLIS with quantitative feedback controller.

The quantitative feedback controller imposes frequency-domain specifications as follows;
1) Tracking, given by;

$$\alpha \le |y/r| = |PGF/(1+PG)| \le \beta, \tag{10}$$

2) Plant-output disturbance rejection, given by;

$$|y/d_O| = |1/(1+PG)| < \delta_{dO}, \tag{11}$$

3) Plant-input disturbance rejection, given by;

$$|y/d_I| = |P/(1+PG)| < \delta_{dI}, \tag{12}$$

4) Noise rejection, given by;

$$|y/n| = |PG/(1+PG)| < \delta_n, \tag{13}$$

where δ_{dO}, δ_{dI}, and δ_n are small positive numbers, and α and β are transfer functions or numbers close to one. The plant-output disturbance and noise rejection specifications are also called *stability margin* specifications due to their direct relationships to the gain and phase stability margins.

Consider again the underdamped plant $P(s) = \omega_n^2/(s^2 + 2\zeta\omega_n s + \omega_n^2)$, where $\omega_n = 1\ \text{rad.s}^{-1}$ and $\zeta = 0.1$. A PID controller with $k_p = 50$, $k_i = 30$, and $k_d = 1$ and an input shaper with 3 impulses (2),

placed outside of the loop as in **Figure 2** and designed using a closed-loop natural frequency $\omega_n = 7.116$ rad.s^{-1} and damping ratio $\zeta = 0.043$, deliver the simulation result as shown in **Figure 5**. **Figure 5** for OLIS is comparable to **Figure 3** for CLSS. As expected, only the vibration induced by the reference can be handled by the outside-of-the-loop input shaper. The input shaper has no effects on the vibrations induced by other sources; it is the job of the feedback controller to handle them.

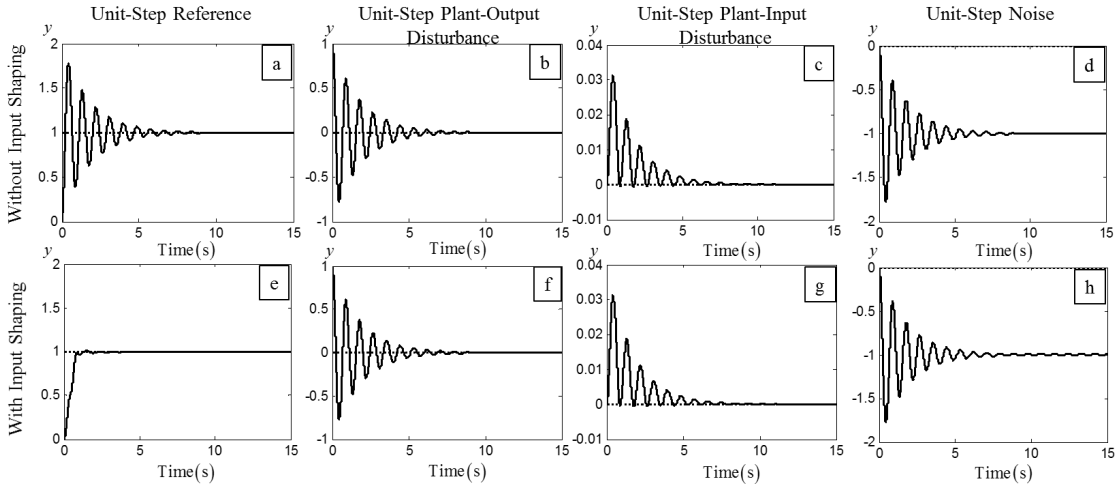

Figure 5 OLIS. a) to d) are the outputs y due to unit-step reference, unit-step plant-output disturbance, unit-step plant-input disturbance, and unit-step noise, respectively, without input shaping. e) to h) are those with input shaping. The solid lines are the output *y*, and the dotted lines are the reference *r*.

Next, we will design the quantitative feedback controller for the underdamped example plant. Our frequencies of interest are 0.5, 1, 1.5, 5, and 9 rad.s^{-1} because they are around the plant's natural frequency. The plant parameters ω_n and ζ are allowed to have uncertainties ranging from $0.9 \le \omega_n \le 1.1$ and $0.08 \le \zeta \le 0.12$. The control system will ensure all specifications will be met for these uncertainties in the plant model. **Figure 6** shows uncertain regions of the plant, so-called *plant templates*, at the frequencies of interest: 0.5, 1, 1.5, 5, and 9 rad.s^{-1}, on the Nichols chart. The plant templates cover all the uncertainties in the plant parameters ω_n and ζ.

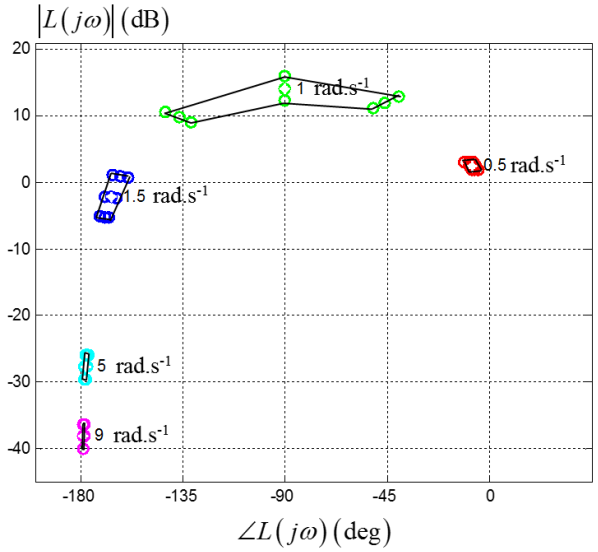

Figure 6 Plant templates at 5 frequencies of interest.

Design parameters in the specifications (10) - (13) are as follows: $\delta_{dO} = \delta_{dI} = \delta_n = 7$ dB, $\alpha = [-0.5, -1, -3, -8, -14]$ dB and $\beta = [0.5, 1, 2, 3, 4]$ dB, for frequencies 0.5, 1, 1.5, 5, and 9 rad.s^{-1}, respectively. Notice that we relax the tracking specifications to emphasize fast response rather than low overshoot because the overshoot will be handled by the input shaper by reducing vibration induced by the reference input. All specifications are converted to bounds. For each frequency, all bounds are integrated, producing a worst-case bound. The controller $G(s)$ will be designed such that the open-loop shape $L(s) = P(s)G(s)$ lies above or outside of each worst-case bound for all interested frequencies.

Figure 7 shows the open-loop shape $L(s)$ and worst-case bounds, when the PID controller used in producing the simulation result in **Figure 5** is used. The worst-case bounds were generated from the frequency-domain specifications (10) - (13). We see that all specifications are met except at 5 and 9 rad.s^{-1}, whose violations cause high oscillations in the result.

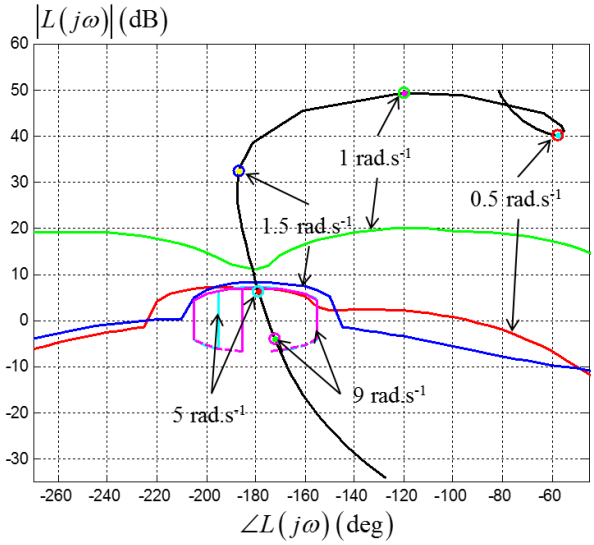

Figure 7 Open-loop shape with the previous PID controller together with worst-case specification bounds.

A loop shaping is performed by appending a lead to meet all specifications. **Figure 8** shows the appending result. The controller changes from the PID controller $G(s)=30(s/49.39+1)(s/0.61+1)/s$ to;

$$G(s)=\frac{30\left(\frac{s}{49.39}+1\right)\left(\frac{s}{0.61}+1\right)\left(\frac{s}{2.54}+1\right)}{s\left(\frac{s}{7.97}+1\right)}. \tag{14}$$

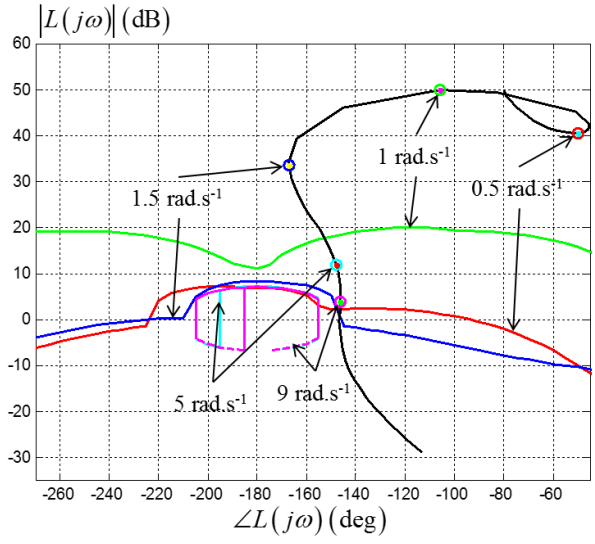

Figure 8 Open-loop shape after loop shaping by adding a lead.

Figure 9 shows the design of the prefilter $F(s)$. The 2 dashed lines are the tracking upper and lower bounds. The 2 solid lines are closed-loop transfer function magnitudes, $|PGF/(1+PG)|$, for 2 worst plant variation cases. Because the input shaper takes care of the vibration induced by reference input, the only purpose of the prefilter $F(s)$ is to ensure steady-state tracking. From **Figure 9**, the low-frequency gain is already at 0 dB, so the prefilter $F(s)$ was left as 1.

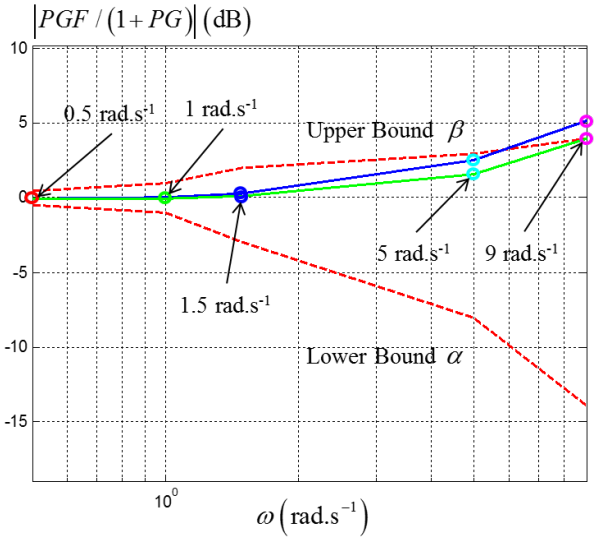

Figure 9 Prefilter design.

Figures 10a - 10d show the specifications (10) - (13), respectively. The asterisks mark the upper and lower bounds of each specification for the frequencies of interest: 0.5, 1, 1.5, 5, and 9 rad.s^{-1}. One solid line represents each plant in the plant uncertainty set. All specifications, except the tracking at 5 and 9 rad.s^{-1}, are met for all plant uncertainties and all frequencies.

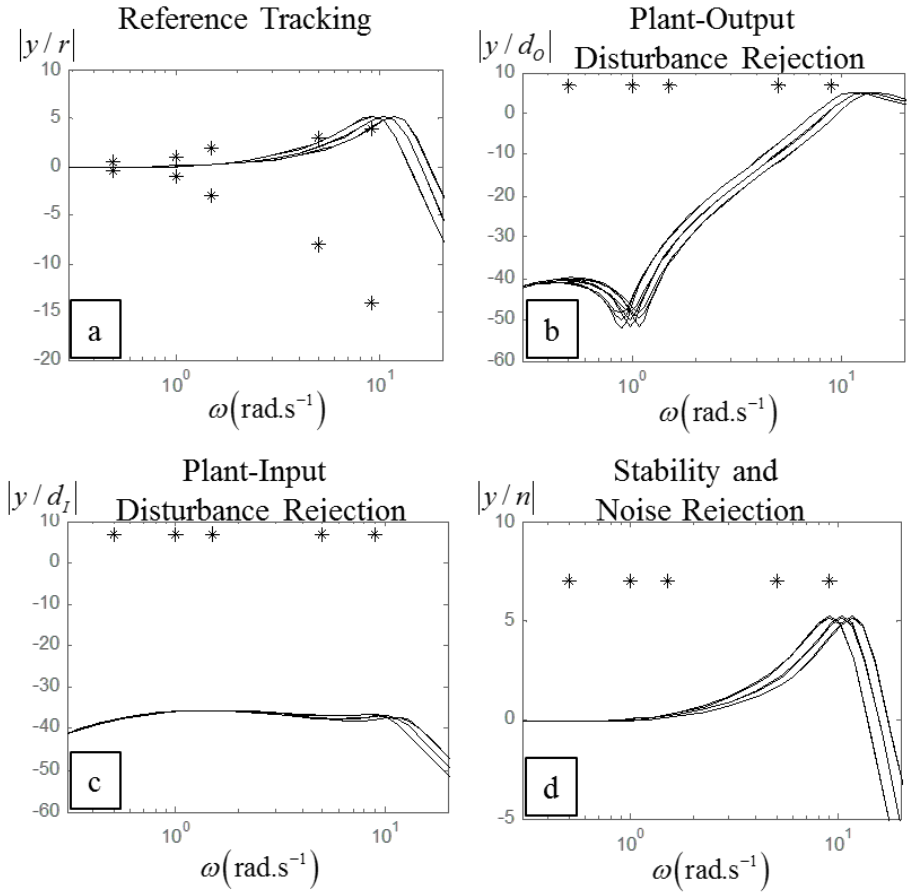

Figure 10 Frequency-domain specifications: a) reference tracking; b) plant-output disturbance rejection; c) plant input disturbance rejection; and d) stability and noise rejection.

The 3-impulse input shaper (2), designed using closed-loop natural frequency $\omega_n = 11.731\,\text{rad.s}^{-1}$ and damping ratio $\zeta = 0.331$, is used.

Figure 11 contains the simulation result in the time domain using the control system in **Figure 4**. **Figure 11** for the proposed system is comparable to **Figure 5** for OLIS and **Figure 3** for CLSS. By comparing **Figure 11** to **Figure 5**, the control system reduces vibrations from all sources well. By comparing **Figures 11e - 11a**, the input shaper helps reduce the vibration as seen from the lower overshoot and faster settling time.

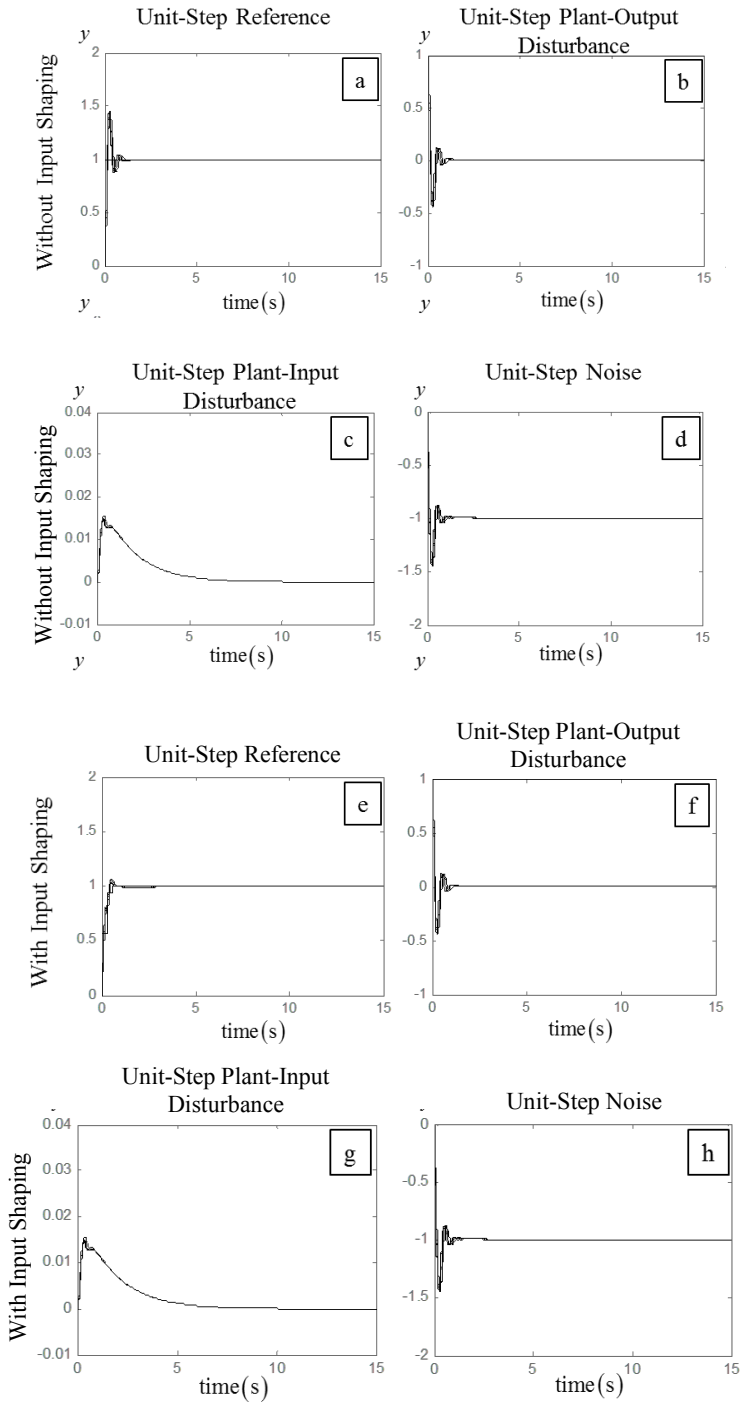

Figure 11 Simulation of OLIS. a) to d) are the outputs y due to unit-step reference, unit-step plant-output disturbance, unit-step plant-input disturbance, and unit-step noise, respectively, without input shaping. e) to h) are those with input shaping. The solid lines are the output y, and the dotted lines are the reference r.

Results and discussion

In this section, the results on implementing the proposed technique with a 2-staged pendulum are presented. Consider a diagram of a 2-staged pendulum in **Figure 12**. The pendulum system consists of a slider, 2 rigid links, and a payload. A linear motor drives the pendulum system. The objective is to move the payload from point to point, back and forth, as fast as possible. This can be achieved only when the oscillations of the links are minimized. The parameters in **Figure 12** are given in **Table 1**.

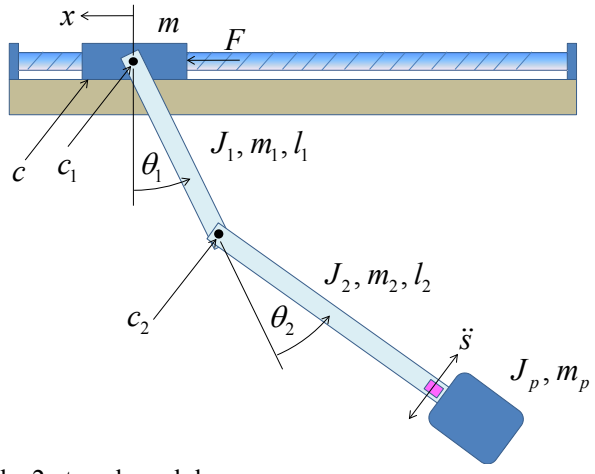

Figure 12 Schematic of the 2-staged pendulum.

Three equations of motion are given by;

$$\begin{aligned}
&m\ddot{x}+m_1\left(\ddot{x}-\frac{l_1}{2}\ddot{\theta}_1\right)+m_2\left(\ddot{x}-l_1\ddot{\theta}_1-\frac{l_2}{2}\ddot{\theta}_2\right)+m_p\left(\ddot{x}-l_1\ddot{\theta}_1-l_2\ddot{\theta}_2\right)\\
&-m_1\left(\ddot{x}-\frac{l_1}{2}\ddot{\theta}_1\right)\frac{l_1}{2}+J_1\ddot{\theta}_1-m_2\left(\ddot{x}-l_1\ddot{\theta}_1-\frac{l_2}{2}\ddot{\theta}_2\right)l_1+J_2\left(\ddot{\theta}_1+\ddot{\theta}_2\right)
\end{aligned} = F-c\dot{x},$$

$$\begin{aligned}
&-m_p\left(\ddot{x}-l_1\ddot{\theta}_1-l_2\ddot{\theta}_2\right)l_1+J_p\left(\ddot{\theta}_1+\ddot{\theta}_2\right)+m_1g\frac{l_1}{2}\sin\theta_1+m_2gl_1\sin\theta_1\\
&+m_2g\frac{l_2}{2}\sin\left(\theta_1+\theta_2\right)+m_pgl_1\sin\theta_1+m_pgl_2\sin\left(\theta_1+\theta_2\right)
\end{aligned} = -c_1\dot{\theta}_1, \qquad (15)$$

$$\begin{aligned}
&-m_2\left(\ddot{x}-l_1\ddot{\theta}_1-\frac{l_2}{2}\ddot{\theta}_2\right)\frac{l_2}{2}+J_2\left(\ddot{\theta}_1+\ddot{\theta}_2\right)-m_p\left(\ddot{x}-l_1\ddot{\theta}_1-l_2\ddot{\theta}_2\right)l_2\\
&+J_p\left(\ddot{\theta}_1+\ddot{\theta}_2\right)+m_2g\frac{l_2}{2}\sin\left(\theta_1+\theta_2\right)+m_pgl_2\sin\left(\theta_1+\theta_2\right)
\end{aligned} = -c_2\dot{\theta}_2.$$

where parameters and their values from an actual experimental hardware are given in **Table 1**.

Table 1 Parameters and their values for the 2-staged pendulum based on the actual experimental hardware.

Parameter	Description	Values in S.I. unit
J_1, J_2, J_p	Links and payload mass moment of inertia about C.G.	7.5×10^{-4}, 0.0082, 0.001
m, m_1, m_2, m_p	Slider, links, and payload mass	0.1, 0.1, 0.2, 0.2
l_1, l_2	Links length	0.3, 0.7
c, c_1, c_2	Slider and links friction coefficients	1, 0.01, 0.01
F	Push force from screw	

By lumping all masses together and treating oscillation of the links and payload as plant-input disturbance, which will be attenuated by the control system, a simple second-order model is obtained as;

$$M\ddot{x} + c\dot{x} = F + O_x, \tag{16}$$

where $M = m + m_1 + m_2 + m_p$ and O_x is the force disturbance resulting from oscillations of the links and payload given by;

$$O_x = m_1\ddot{\theta}_1\frac{l_1}{2} + m_2\left(\ddot{\theta}_1 l_1 + \ddot{\theta}_2\frac{l_2}{2}\right) + m_p\left(\ddot{\theta}_1 l_1 + \ddot{\theta}_2 l_2\right). \tag{17}$$

It can be shown that this simplified model with disturbance is identical to the true model (15) when $\sin\theta \approx \theta$.

The quantitative feedback controller is designed on the plant (16). By allowing M and c to have $\pm10\%$ variations from their nominal values, the plant templates at 0.1, 0.5, 1, 3, and 8 rad.s^{-1} are shown in **Figure 13**. Note that, for clarity, only 5 frequencies are displayed when the design includes more frequencies ranging from 0.1 to 100 rad.s^{-1}.

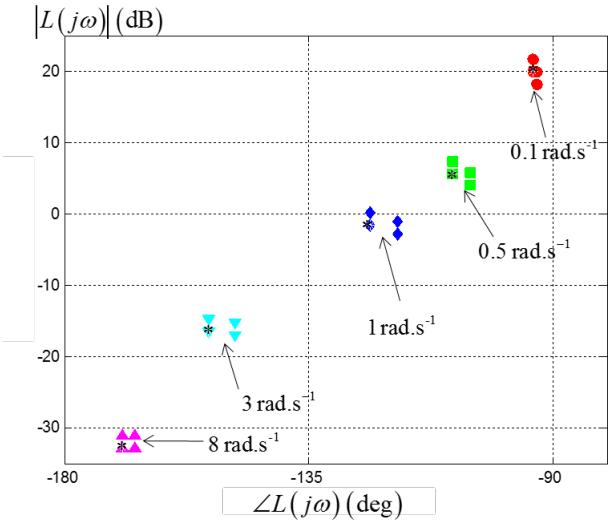

Figure 13 Plant templates at 5 frequencies of interest.

The design specifications Eqs. (10) - (12) are selected to be $\alpha = 24.75/\left(s^2+10s+25\right)$, $\beta = 101/\left(s^2+14s+100\right)$, $\delta_{dO} = 4$ dB, and $\delta_{dI} = -15$ dB. The specifications are converted to bounds and are integrated to produce worst-case bounds for all 5 frequencies as shown in **Figure 14**, where the symbol ① indicates the plant-input disturbance rejection bound, ② indicates the plant-output disturbance rejection bound, and ③ indicates the tracking bound. The solid line is the final open-loop shape for the controller $G = \left[1955.8085\left(s+1.616\right)\right]/\left[\left(s+17.46\right)\left(s+29.17\right)\right]$ and the prefilter $F = 6.0688/\left(s+6.069\right)$.

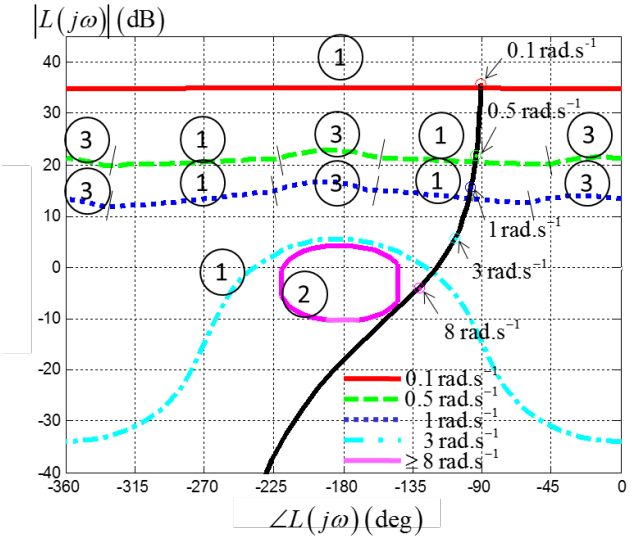

Figure 14 Open-loop shape after loop shaping.

In designing the input shaper, the closed-loop natural frequencies and damping ratios are obtained from the true model (15) with $\sin\theta \approx \theta$ and the controller and prefilter obtained previously. The natural frequencies of the underdamped modes are $\omega_1 = 2.83$ rad.s^{-1}, $\omega_2 = 6.82$ rad.s^{-1}, and $\omega_3 = 17.1$ rad.s^{-1}. The corresponding damping ratios are $\zeta_1 = 9.35\times10^{-2}$, $\zeta_2 = 2.15\times10^{-1}$, and $\zeta_3 = 8.13\times10^{-2}$. One 3-impulse input shaper (2) is used per one natural frequency and damping ratio.

The simulation results are obtained from applying the proposed control system in **Figure 4** to the true model (15) of the 2-stage pendulum. **Figure 15a** shows the result of using a well-tuned PID controller without the input shaper by comparing the payload position, which is computed from x, θ_1, and θ_2 to be $x - l_1\theta_1 - \left(l_1+l_2\right)\theta_2$, to a square-wave reference input. **Figure 15b** shows the result of using the designed quantitative feedback controller above with the input shaper. It can be seen that the payload vibration, as a result of moving the pendulum from point to point, is reduced significantly. The 3 % settling time is also reduced from 17 to 4 s.

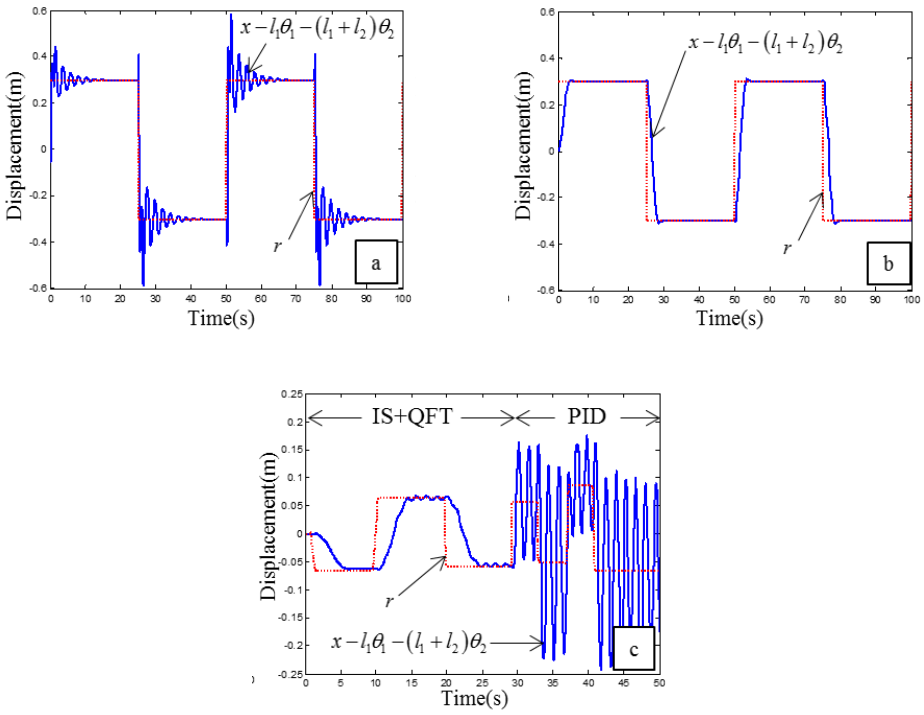

Figure 15 Payload position and its reference: a) simulation result using PID controller without input shaper; b) simulation result using quantitative feedback controller with input shaper; and c) experimental result.

Experimental results are obtained from implementing the control system in **Figure 4** with a laboratory-scale 2-stage pendulum, controlled by a human as shown in **Figure 16a**. **Figure 16b** contains a diagram of the experimental arrangement. Two optical encoders measure the relative angular positions θ_1 and θ_2 of the links. Another optical encoder, attached to the motor, measures motor shaft's angular position, which can be converted to the slider's linear position x. An uncertain payload container, carrying some movable coins, is placed at the tip. An accelerometer is attached near the payload to measure its linear acceleration. A host computer, running Labview and Matlab software, is used to communicate with the user and a target computer. Matlab is used for off-line analysis and simulation. The real-time hardware-in-the-loop experiment is performed using Labview. The sampling time of 1 ms is used for the hardware. The same quantitative feedback controller, input shaper, and PID controller as those for simulation are used. **Figure 15c** plots the pendulum's payload position, $x-l_1\theta_1-(l_1+l_2)\theta_2$, versus its desired trajectory given arbitrarily by the human operator. By switching from the proposed quantitative feedback controller with input shaper to the unshaped PID controller, the payload experiences severe residual vibration.

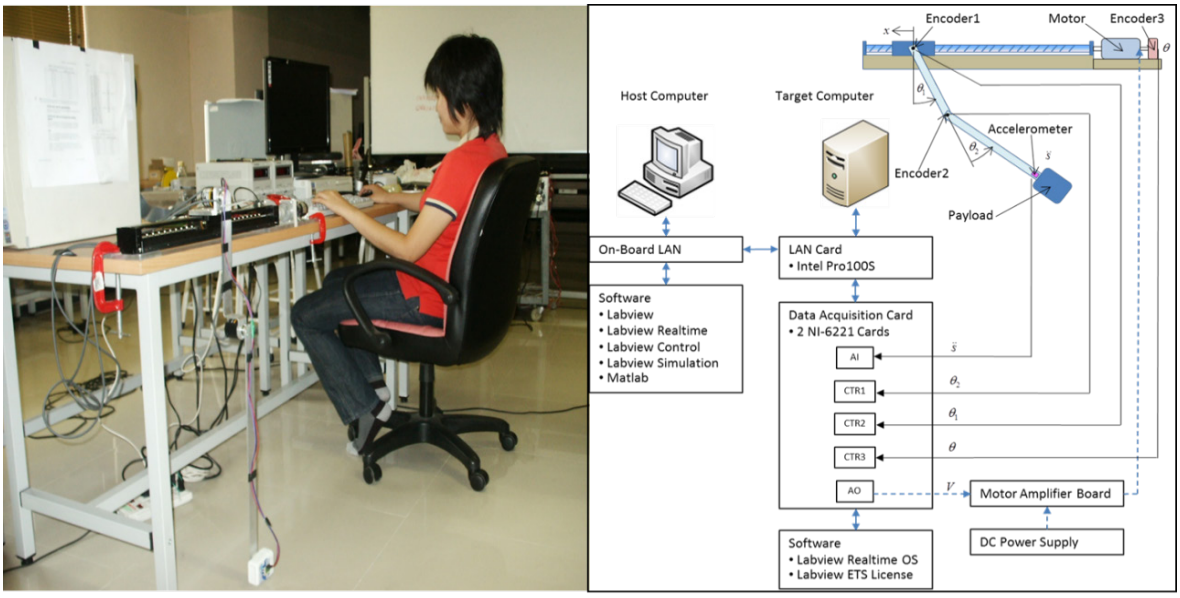

(a) (b)

Figure 16 Experimental set-up (a) the laboratory-scaled 2-staged pendulum and (b) connection diagram.

Placing the input shaper in the feedback loop as in the closed-loop signal shaping system shown in **Figure 1** is shown to reduce vibration induced by the reference, plant-output disturbance, and noise as shown in the simulation result in **Figure 3**. However, the input shaping filter contains time delays that limit the performance of the feedback controller when placed in the feedback loop. Placing the input shaper outside of the loop as in the outside-the-loop input shaping system shown in **Figure 2** only suppresses the vibration induced by the reference as shown in the simulation result in **Figure 5**. This paper proposes combining the outside-the-loop input shaping with a quantitative feedback control. The proposed system is shown in **Figure 4**. The quantitative feedback control can be designed to handle vibrations induced by the plant-output disturbance, plant-input disturbance, noise, as well as reference, as shown in the simulation result in **Figure 11**. **Figure 15** contains the simulation result from using the proposed system with a 2-stage pendulum. **Figure 15** also includes the experimental result, which shows the effectiveness of the proposed system.

Conclusions

An input shaper and feedback controller normally work together in a closed-loop system. When placed outside of the loop, the input shaper only reduces vibrations induced by the reference input. The feedback controller must therefore handle vibrations from other sources such as external disturbances, noise, and uncertainty. The feedback controller also is responsible for obtaining good tracking and system stability.

The quantitative feedback controller is suitable for being used as the feedback controller. This type of controller is designed to meet several frequency-domain specifications for all plants in the uncertain plant set. The control designer can quantitatively evaluate the tradeoffs among tracking, disturbances rejection, noise rejection, and stability margin. As a result, the feedback controller is guaranteed to reduce vibrations from other sources and to deliver good tracking and system stability.

As far as we know, using QFT with input shaping has not been done before by other groups of researchers. The merits of the proposed combination of the input shaping and quantitative feedback control methods are as follows: 1) No time delay is added to the closed-loop system because the input

shaper is placed outside of the loop; 2) Vibrations induced by disturbances, noise, nonlinearities, and initial conditions can be suppressed by the quantitative feedback control whereas vibrations induced by the reference signal can be suppressed by the input shaper. However, since the quantitative feedback control is effective as a single-input-single-output (SISO), the proposed system is likely to find some difficulties in the case of flexible plants with a multi-input-multi-output (MIMO) system.

The focus of this paper is on using a quantitative feedback control to enhance the input shaping. In general, IS should enable QFT to be more aggressive in tracking of the system with lightly damped poles. However, whether QFT alone can be designed to outperform QFT+IS is a very interesting subject of its own which requires extensive research beyond the main idea of this work and will be the subject of future work. Future work is to use the quantitative feedback controller in model matching task. The closed-loop system, consisting of the controller and a plant, can be designed to match the reference model. Then, the input shaper, placed outside of the loop, can be designed to suppress vibrations for the reference model.

Acknowledgements

The author would like to thank Craig Borghesani and Terasoft, Inc for their evaluation copy of the QFT Matlab toolbox.

References

[1] NC Singer and WC Seering. Preshaping command inputs to reduce system vibration. *J. Dyn. Syst. Meas. Contr.* 1990; **112**, 76-82.
[2] OJM Smith. Posicast control of damped oscillatory systems. *Proc. IRE* 1957; **45**, 1249-55.
[3] GH Tallman and OJM Smith. Analog study of dead-beat posicast control. *IRE T. Automat. Contr*. 1958; **4**, 14-21.
[4] W Singhose. Command shaping for flexible systems: A review of the first 50 years. *Int. J. Precis. Eng. Manuf.* 2009; **10**, 153-68.
[5] JR Huey and W Singhose. Trends in the stability properties of CLSS controllers: A root-locus analysis. *IEEE Trans. Contr. Syst. Tech*. 2010; **18**, 1044-56.
[6] J Stergiopoulos and A Tzes. Hinf closed-loop control for uncertain discrete input-shaped systems. *J. Dyn. Syst. Meas. Contr.* 2010; **132**, 1-8.
[7] V Kapila, A Tzes and Q Yan. Closed-loop input shaping for flexible structures using time-delay control. *J. Dyn. Syst. Meas. Contr.* 2000; **122**, 454-60.
[8] U Staehlin and T Singh. Design of closed-loop input shaping controllers. *In*: Proceeding of the American Control Conference, Denver, Colorado, 2003, p. 5167-72.
[9] K Zuo and D Wang. Closed loop shaped-input control of a class of manipulators with a single flexible link. *In*: Proceeding of the IEEE International Conference on Robotics and Automation, Nice, France, 1992, p. 782-7.
[10] A Zolfagharian, A Noshadi, MZM Zain and ARA Bakar. Practical multi-objective controller for preventing noise and vibration in an automobile wiper system. *Swarm Evol. Comput.* 2013; **8**, 54-68.
[11] FM Aldebrez, MS Alam and MO Tokhi. Input-shaping with GA-tuned PID for target tracking and vibration reduction. *In*: Proceeding of the Mediterranean Conference on Control and Automation, Limassol, Cyprus, 2005, p. 485-490.
[12] MC Pai. Robust input shaping control for multi-mode flexible structures using neuro-sliding mode output feedback control. *J. Frankl. Inst*. 2012; **349**, 1283-303.
[13] Q Hu, XZ Gao and G Ma. Reference model variable structure output feedback for attitude maneuvers control of flexible spacecrafts. *Intell. Autom. Soft Comput*. 2009; **15**, 53-62.
[14] JR Huey and W Singhose. Design of proportional-derivative feedback and input shaping for control of inertia plants. *IET Control Theory A* 2012; **6**, 357-64.
[15] M Kenison and W Singhose. Concurrent design of input shaping and proportional plus derivative feedback control. *J. Dyn. Syst. Meas. Contr.* 2002; **124**, 398-405.

[16] AG Dharne and S Jayasuriya. Increasing the robustness of the input-shaping method using adaptive control. *In*: Proceeding of the American Control Conference, Denver, Colorado, 2003, p. 1578-83.
[17] JR Huey, KL Sorensen and WE Singhose. Useful applications of closed-loop signal shaping controllers. *Contr. Eng. Pract*. 2008; **16**, 836-46.
[18] S Skogestad and I Postlethwaite. *Multivariable Feedback Control*. John Wiley and Sons, New York, 2005.
[19] O Yaniv. *Quantitative Feedback Design of Linear and Nonlinear Control Systems*. Springer, New York, 1999.